International Journal of Nanomedicine

Dovepress
open access to scientific and medical research

Open Access Full Text Article

ORIGINAL RESEARCH

Gold nanoparticles-loaded hydroxyapatite composites guide osteogenic differentiation of human mesenchymal stem cells through Wnt/β-catenin signaling pathway

This article was published in the following Dove Press journal:
International Journal of Nanomedicine

Hang Liang[1,*]
Xiaomo Xu[2,*]
Xiaobo Feng[1]
Liang Ma[1]
Xiangyu Deng[1]
Shuilin Wu[2,3]
Xiangmei Liu[2]
Cao Yang[1]

[1]Department of Orthopaedics, Union Hospital, Tongji Medical College, Huazhong University of Science and Technology, Wuhan 430022, People's Republic of China; [2]Hubei Key Laboratory of Polymer Materials, School of Materials Science & Engineering, Ministry-of-Education Key Laboratory for the Green Preparation and Application of Functional Materials, Hubei University, Wuhan 430062, People's Republic of China; [3]School of Materials Science & Engineering, the Key Laboratory of Advanced Ceramics and Machining Technology by the Ministry of Education of China, Tianjin University, Tianjin 300072, People's Republic of China

*These authors contributed equally to this work

Correspondence: Xiangmei Liu
School of Materials Science & Engineering, Ministry-of-Education Key Laboratory for the Green Preparation and Application of Functional Materials, Hubei University, Wuhan 430062, People's Republic of China
Tel +860 278 866 1729
Email liuxiangmei1978@163.com

Cao Yang
Department of Orthopaedics, Union Hospital, Tongji Medical College, Huazhong University of Science and Technology, Wuhan 430022, People's Republic of China
Tel +86 0 278 572 6114
Email yangcao1971@sina.com

Background: Precise control and induction of the differentiation of stem cells to osteoblasts by artificial biomaterials are a promising strategy for rapid bone regeneration and reconstruction.

Purpose: In this study, gold nanoparticles (AuNPs)-loaded hydroxyapatite (HA-Au) nanocomposites were designed to guide the osteogenic differentiation of human bone marrow-derived mesenchymal stem cells (hMSCs) through the synergistic effects of both AuNPs and HA.

Materials and methods: The HA-Au nanoparticles were synthesized and characterized by several analytical techniques. Cell viability and proliferation of hMSCs were characterized by CCK-8 test. Cellular uptake of nanoparticles was observed by transmission electron microscope. For the evaluation of osteogenic differentiation, alkaline phosphatase (ALP) activity and staining, Alizarin red staining, and a quantitative real-time polymerase chain reaction (RT-PCR) analysis were performed. In order to examine specific signaling pathways, RT-PCR and Western blotting assay were performed.

Results: The results confirmed the successful synthesis of HA-Au nanocomposites. The HA-Au nanoparticles showed good cytocompatibility and internalized into hMSCs at the studied concentrations. The increased level of ALP production, deposition of calcium mineralization, as well as the expression of typical osteogenic genes, indicated the enhancement of osteogenic differentiation of hMSCs. Moreover, the incorporation of Au could activate the Wnt/β-catenin signaling pathway, which seemed to be the molecular mechanism underlying the osteoinductive capability of HA-Au nanoparticles.

Conclusion: The HA-Au nanoparticles exerted a synergistic effect on accelerating osteogenic differentiation of hMSCs, suggesting they may be potential candidates for bone repair and regeneration.

Keywords: gold nanoparticles, hydroxyapatite, nanocomposites, osteoblast differentiation, bone regeneration

Introduction

Many critical bone defects arising from high-energy trauma, congenital malformations, infection or tumor resection can seldom be repaired by self-healing, thus eventually result in limb discrepancy, deformation, and dysfunction.[1,2] Plenty of research has focused on methods to accelerate the reconstruction or repair of damaged bone tissues.[3] Due to rapid advancement in nanoscience and nanotechnology in the past decades,

nanoparticle-based biomaterials have been attracting extensive attention in the field of tissue engineering, biological technology, and biomedical sciences.[4–6] Among these nanoparticles, hydroxyapatite (HA) is one of the most popular biomaterials in many biomedical applications, especially in bone tissue engineering.[7–9] This is because its inorganic component is similar to the native bone matrix, which endows this material with outstanding biocompatibility, osteoinductivity, osteoconductivity, bone-bonding ability, and excellent biodegradability.[10–12] However, HA is not able to completely satisfy the demands of regenerative medicine for bone repair. The limited ability of HA to mobilize endogenous stem cells in order to guide autologous bone tissue regeneration limits the expansion of its application in the field of bone tissue engineering.[13] Therefore, it is necessary to develop new efficient HA-based nanocomposites to address these problems.

Gold nanoparticles (AuNPs) have been considered to be prominent nanomaterials in the field of biomedicine, due to their unique optical properties, superior biocompatibility, facile synthesis method, and various strategies for surface modification.[14–17] Various nanocomposites based on AuNPs have been synthesized for biological imaging, targeted drug and gene delivery, photothermal and photodynamic therapy, biosensors and tissue engineering.[6,18–21] Moreover, increasing evidence suggests that AuNPs are promising osteoinductive biomaterials for bone tissue engineering and regeneration.[22–25] It was found that AuNPs induced osteogenic differentiation of human bone marrow-derived mesenchymal stem cells (hMSCs), inhibition of adipogenic differentiation after endocytosis into the cytoplasm and mitogen-activated protein kinase signaling pathway played an important role in this process.[22] In addition, chitosan-conjugated AuNPs with different concentrations also had osteoinductive capability to guide differentiation of human adipose-derived stem cells (ADSCs) to osteoblasts.[23] Similarly, osteogenic activity and mineralization of osteoblasts could be significantly enhanced by AuNPs.[24,25] However, it is noteworthy that the properties of AuNPs, particularly the size and shape, have a great effect on the osteoinductive capability of AuNPs.[24,26,27] Ko et al , investigated the effect of various sizes (15, 30, 50, 75, and 100 nm) of Au nanoparticles on the osteogenic differentiation of ADSCs and finally demonstrated that 30 and 50 nm AuNPs appeared to be more efficient in promoting differentiation of ADSCs to osteoblasts than the other sizes studied.[26] Conversely, it has been reported that the AuNPs with 20 nm diameter had more positive effects on osteogenic differentiation toward osteoblasts than the AuNPs with 40 nm diameter.[24] Moreover, Li et al, reported that the shape as well as the size of AuNPs exert significant effects on the osteogenic differentiation in stem cells.[27] Au nanospheres with 40 and 70 nm diameters and Au nanorods with 70 nm diameter significantly enhanced the differentiation of hMSCs to osteoblasts while Yes-associated proteins played an important role in this process. However, another study reported that although AuNPs with 45 nm diameter enhanced the differentiation of stem cells into osteoblasts the most compared with other smaller sizes, AuNPs with 5 nm diameter did not show any osteoinductive capability, and even significantly blocked osteogenic differentiation.[28] These facts indicate that the osteoinductive properties of AuNPs with various sizes and shapes are quite different and further research is needed to improve the performance of AuNPs for bone regeneration and tissue engineering.

Accordingly, in this study, we aimed to develop multifunctional AuNPs-loaded HA (HA-Au) nanocomposites in order to combine the merits of the two materials to achieve a synergistic effect of accelerating the osteogenic differentiation of hMSCs. In this study, we synthesized and characterized the novel HA-Au nanocomposites for the first time. Then, the cytocompatibility and osteogenic efficacy of the HA-Au nanoparticles in hMSCs were evaluated. The potential molecular mechanism of HA-Au nanocomposites-mediated osteogenic differentiation was also investigated. The results clearly revealed that HA-Au nanoparticles can synergistically promote differentiation of hMSCs to osteoblasts, which suggests that HA-Au nanoparticles might be a promising therapeutic candidate as a bone regenerative nanomaterial for bone repair. The preparation process and related mechanism are illustrated in Scheme 1.

Materials and methods

Preparation of HA-Au nanoparticles

In this study, Au-loaded HA nanoparticles were synthesized in the same way as our previous study.[29] Briefly, the HA nanoparticles were obtained using a hydrothermal method. Calcium nitrate tetrahydrate ($Ca(NO3)_2•4H_2O$) and di-ammonium hydrogen phosphate ($(NH_4)_2HPO_4$) were mixed in aqueous solution. Then, 25% ammonium hydroxide solution was used for pH adjustment. After that, the mixture was heated, washed, freeze-dried, and calcined. On the other hand, the AuNPs were loaded on HA nanoparticles by a deposition–precipitation method.

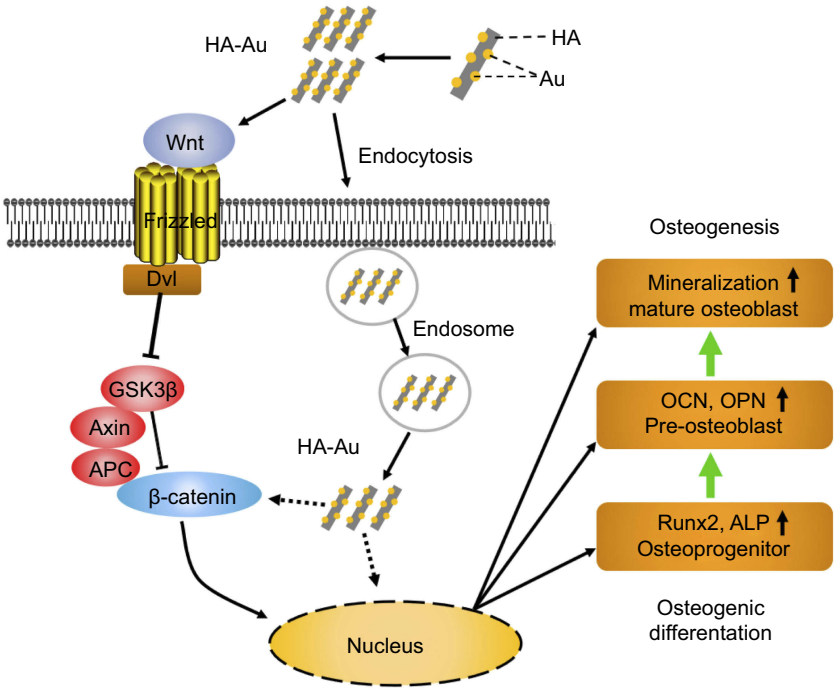

Scheme 1 Schematical illustration showing the possible molecular mechanism for enhanced osteogenesis by HA-Au nanoparticles by activation of Wnt/β-catenin signaling pathway as well as internalization into the hMSCs.
Abbreviations: HA-Au, gold nanoparticles-loaded hydroxyapatite; hMSCs, human bone marrow-derived mesenchymal stem cells.

$HAuCl_4 \cdot 3H_2O$ were dissolved in deionized water at a pH of 9 by adding 0.1 M NaOH. Then, the HA nanoparticles were mixed with the aqueous solution of $HAuCl_4$. After stirring and heating, the product was washed, lyophilized, and calcined. The HA-Au nanoparticles were divided into two groups based on the different contents of AuNPs (low and high content were labeled as HA-Au1 and HA-Au2, respectively).

Characterization of HA-Au nanoparticles

Transmission electron microscope (TEM; Tecnai G20 electron microscope, FEI, USA) was performed to determine the microstructure and the morphologies of the HA and HA-Au nanoparticles. X-ray powder diffractometry (XRD, D8A25, Bruker, Germany) was used to determine the crystallinity and purity of the nanoparticles. Fourier-transformed infrared spectroscopy (FTIR, Nicolet IS10, USA) and X-ray photoelectron spectroscopy (XPS, ESCALAB 250Xi, Thermo Fisher Scientific, USA) were used to measure the chemical compositions and chemical states of the nanoparticles.

Culture of hMSCs

hMSCs were purchased from Cyagen Biosciences, USA. The hMSCs were plated in 75 cm^2 tissue culture flasks and cultured in the stem cell growth medium (Cyagen Biosciences, USA) at 37°C with 5% CO_2. The medium was replaced every 3 days during cell culturing. After growing to sub-confluence, cells were collected using Trypsin-EDTA (0.25%), centrifuged, and resuspended in growth medium for reseeding in new culture flasks. Cells were used for further study after two to five passages. For osteogenic induction, cells were trypsinized and cultured in the growth medium overnight. After cells adherence, the medium was changed to an osteogenic induction medium (Cyagen Biosciences, USA) containing phosphate buffer saline (PBS), HA or HA-Au nanoparticles, respectively. For the mechanism experiments, the hMSCs were pre-treated with 10 μM ICG-001, one of the Wnt/β-catenin signaling pathway inhibitors, and subsequently cultured with HA-Au nanoparticles in osteoinductive medium.

Viability and proliferation of hMSCs

Cell Counting Kit-8 (CCK-8; KeyGEN bioTECH, Nanjing, China) was used to determine the viability of hMSCs. Briefly, the hMSCs were seeded in 96-well plates and cultured in growth medium at 37°C with 5% CO_2 overnight. Then, HA-Au and HA nanoparticles were added into plates at a series of concentrations (10, 50, 100, 200 μg/mL). After incubation for 2 days, the cells were washed twice and then

10 μL CCK8 reagent and 100 μL fresh medium were added into each well. The hMSCs were cultured for another 4 hrs in dark at 37°C with 5% CO_2, and subsequently, their absorbance at 450 nm was measured. As for the proliferation assay, the hMSCs were seeded in 96-well plates with growth medium and incubated overnight under the same conditions as the viability assay. Then, the growth medium was replaced with osteogenic induction medium containing HA and HA-Au nanoparticles at a concentration of 100 μg/mL. After incubation for 3 and 7 days, the hMSCs proliferation profile was determined using the CCK-8 (KeyGEN bioTECH, Nanjing, China) assay as described above. The results of cell viability and proliferation are shown as relative percentages compared to the control groups.

Nanoparticles internalization assay

To observe the intracellular localization of HA and HA-Au in hMSCs, the hMSCs were cultured in six-well plate at 37°C with 5% CO_2 for 24 hrs. After refreshing the culture medium containing 100 mg/mL of HA or HA-Au nanoparticles and incubating for 3 days, hMSCs were obtained and fixed using 2.5% glutaraldehyde overnight at 4°C. Then, the cells were post-fixed using 1% osmium tetraoxide for 1 hr at 4°C and then dehydrated stepwise using a series of ethanol concentrations (30%, 50%, 70%, 80%, 90%, 100%). Eventually, the cells were embedded in epoxy resin and sectioned with an ultramicrotome. Ultrathin sections were collected on copper grids to observe the uptake and intracellular distribution of nanoparticles using TEM (Tecnai G20 electron microscope, FEI, USA).

Alkaline phosphatase (ALP) activity assay

ALP Assay Kit (Beyotime, Shanghai, China) was used to measure the ALP activity in hMSCs that were either treated with or without nanoparticles. Based on the information provided in the manufacturer's specifications, the hMSCs were seeded in 24-well plates in growth medium and incubated at 37°C with 5% CO_2. After adherence, the hMSCs were cultured with HA or HA-Au nanoparticles at a concentration of 100 μg/mL in osteoinductive medium for 3, 7, and 14 days. Then, the cells were harvested after washing twice with PBS. The cell suspension from each sample was centrifuged at 1.5×104 rpm to collect the supernatant. After that, the supernatant was added into 96-well plates and co-incubated with p-nitrophenyl phosphate solution for 20 mins. Finally, the reaction was halted by adding stop solution and a microplate reader was used to measure the absorbance corresponding with each sample at a wavelength of 405 nm.

ALP staining

ALP staining Kit (Beyotime, Shanghai, China) was used to determine the intensity of ALP staining in hMSCs treated with or without nanoparticles. The cells were cultured with HA or HA-Au nanoparticles at a concentration of 100 μg/mL in the osteoinductive medium for 3, 7, and 14 days as described above. At the specified time-points, 4% paraformaldehyde was used to fix the hMSCs at room temperature for 20 mins. Then, the fixed cells were washed twice and incubated with ALP staining reagent in accordance with the manufacturer's specifications. The results of ALP activity and staining in hMSCs treated with either HA or HA-Au nanoparticles were showed as relative percentages compared to the control groups.

Calcium deposition assay

Alizarin red S (ARS) staining kit (Cyagen Biosciences Inc., USA) was used to determine the quantity of calcium deposition in hMSCs. The hMSCs were incubated with HA or HA-Au nanoparticles at a concentration of 100 μg/mL in the osteoinductive medium. At the specified time-points (14 and 21 days), 4% paraformaldehyde was used to fix the cells at room temperature. Then, the samples were washed twice with distilled water and treated with ARS staining solution for 20 mins, followed by washing with distilled water and air-drying. The mineralized nodules in each sample were observed using an optical microscope. After that, the stained samples were air-dried and extracted using 10% cetylpyridinium chloride at 25°C for 30 mins. Finally, for quantitative analysis, a microplate reader was used to measure the absorbance corresponding with each sample at a wavelength of 405 nm.

Real-time polymerase chain reaction (PCR) analysis

The expression of marker genes of osteogenic differentiation and Wnt/β-catenin signaling pathway was evaluated using real-time quantitative PCR. The hMSCs were cultured with HA or HA-Au nanoparticles at a concentration of 100 μg/mL treated with or without Wnt/β-catenin inhibitor ICG-001 for 3 and 7 days. Then, the total RNA from each group's cells was collected using TRIzol reagent, extracted using RNAprep pure Cell/Bacteria Kit (TIANGEN, Beijing, China) and transcribed into cDNA

using PrimeScript RT Reagent Kit (Takara Bio, Otsu, Japan). Finally, real-time PCR was performed to amplify the cDNA samples. The results were normalized to β-actin and the 2-ΔΔCt method was used to analyze the mRNA expression levels.

Western blotting analysis

Western blotting assays were performed to test the expression of proteins related to Wnt/β-catenin signaling pathways. Briefly, the hMSCs were cultured with HA or HA-Au nanoparticles at a concentration of 100 μg/mL and with or without Wnt/β-catenin inhibitors for 3 and 7 days. Proteins were extracted using RIPA lysis buffer (Beyotime Institute of Biotechnology) and the concentration was determined using a BCA™ protein assay. Equal amounts of protein were fractionated using gel electrophoresis and blotted onto nitrocellulose membranes. After blocking with 5% nonfat milk, the membranes were incubated overnight with the primary antibody at 4°C. Then, the membranes were washed three times with TBST and incubated with the secondary antibody for 1 hr. Finally, the protein expression was measured using enhanced chemiluminescence reagents. Glyceraldehyde-3-phosphate dehydrogenase protein was used as reference.

Statistical analysis

All data are expressed as mean ± standard deviation (SD). Statistical analysis was performed using Student's *t*-test or one-way analysis of variance. Statistical differences are presented with (*) or (+) for $p<0.05$ and (**) or (++) for $p<0.01$.

Results and discussion

Synthesis and characterization of Au-loaded HA nanoparticles

The Au-loaded HA nanoparticles were synthesized using a deposition–precipitation method. By varying the concentration of $HAuCl_4 \cdot 3H_2O$ in the synthesis process, HA-Au nanoparticles with different Au contents (labeled as HA, HA-Au1, HA-Au2, respectively) were obtained. It was clearly indicated in the TEM images (Figure 1A–C) that the shape of HA nanoparticle was rod measuring about 80–100 nm in length and nearly 20–30 nm in width in all groups. According to the statistical analysis of 200 AuNPs using TEM, the Au nanospheres, with average diameters of 4.7±0.7 nm (Figure 1C), were uniformly distributed in the HA nanoparticles. The amount of Au nanoparticles in HA-Au2 (Figure 1C) was visibly greater than that in HA-Au1 (Figure 1B). The XRD patterns of these nanoparticles are shown in Figure 1D. The diffraction peaks and planes were characteristic of HA (JCPDS: 09–0432).[30] The 2 theta angles of 25.9° correspond to the (002) crystal plane of HA and the three diffraction peaks at 31°–33° correspond to the (211), (112), and (300) crystal plane of HA. As shown in Figure 1E, FTIR spectra tests of the nanoparticles were performed to confirm the presence of HA in all samples. The results revealed that the characteristic bands at 563 and 601 cm^{-1} corresponded to the P–O bending in HA.[31,32] Figure 1F shows the XPS spectra of HA, HA-Au1, and HA-Au2, respectively. Both HA-Au1 and HA-Au2 contain Ca, O, N, C, and Au elements. The high-resolution Au4f spectra of HA-Au1 and HA-Au2 are shown in Figure 1G. These results show that the AuNPs were successfully loaded onto the HA nanorods for both HA-Au1 and HA-Au2 groups.

Cell viability, proliferation, and cellular uptake assay

To investigate the biotoxicity of HA-Au nanoparticles, the viability of hMSCs incubated with HA-Au nanoparticles at varying concentration was analyzed. The viability of the HA, HA-Au1, and HA-Au2 nanoparticles was assessed using the CCK8 assay. As shown in Figure 2A, it was obvious that all the nanoparticles did not have a significant effect on the viability of hMSCs at concentrations of 10, 50, and 100 μg/mL after culturing for 2 days. However, when the concentration of HA-Au nanoparticles increased to 200 μg/mL, the cell viability reduced significantly. These findings indicate that the HA-Au nanoparticles showed cytotoxicity to hMSCs in a concentration-dependent manner. This result was consistent with that of previous reports, which indicated that HA nanocomposites could be safely used at low concentration.[33,34] Based on these results, HA-Au nanoparticles at a concentration of 100 μg/mL, the maximum safe concentration was used in cell proliferation experiments.

In order to further confirm the biocompatibility of HA-Au nanoparticles, we determined the effect of these nanoparticles on the proliferation of hMSCs. After incubation for 3 and 7 days in the osteoinductive medium, the cell number increased in a time-dependent manner in all the experimental groups, indicating that both the HA and HA-Au nanoparticles used in this study had good biocompatibility with hMSCs at the concentration of 100 μg/mL (Figure 2B). In addition, HA-Au2

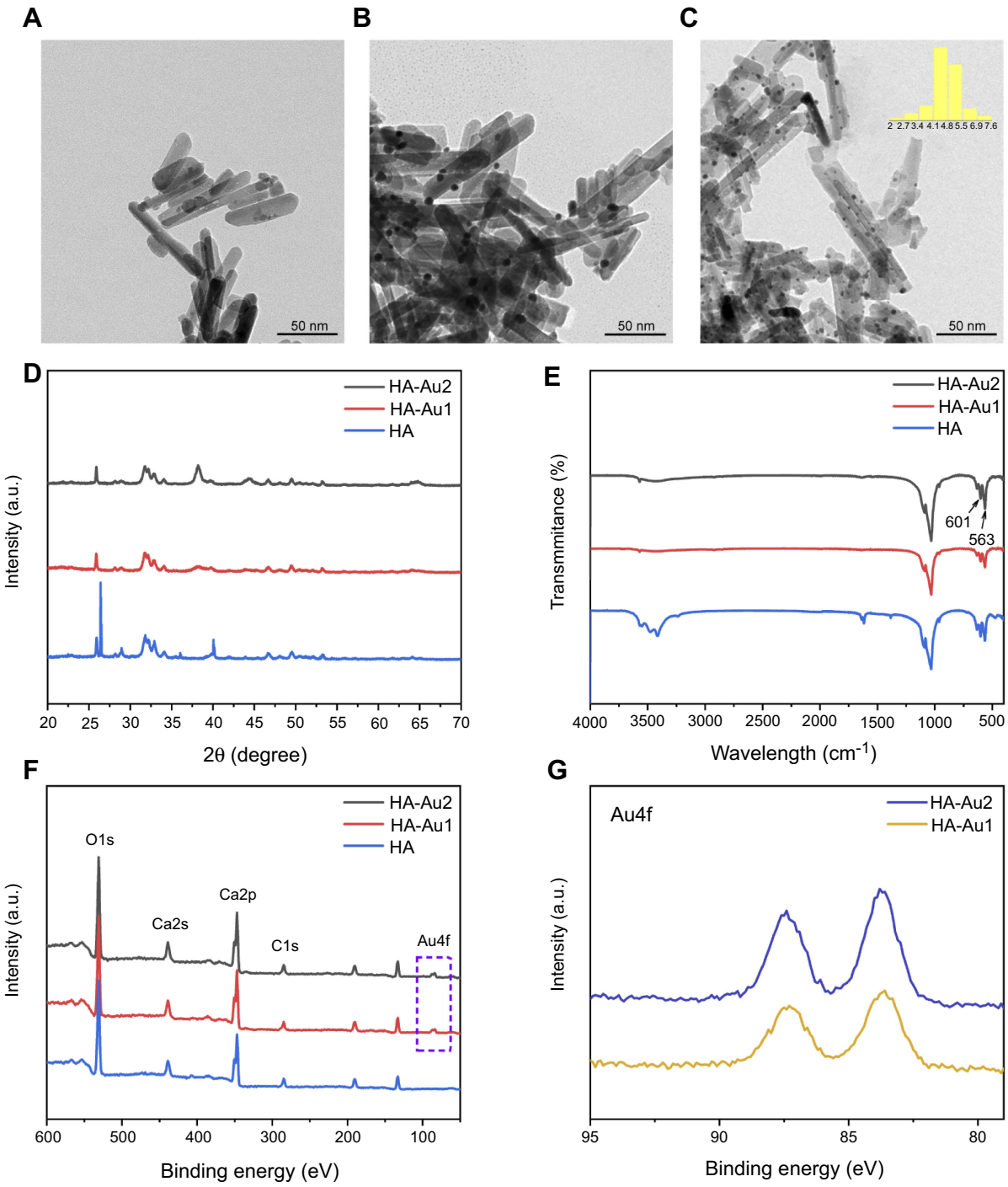

Figure 1 TEM images of (**A**) HA, (**B**) HA-Au1, and (**C**) HA-Au2 (scale bar, 50 nm). (**D**) XRD, (**E**) FT-IR, (**F**) XPS analysis of HA, HA-Au1, and HA-Au2. (**G**) The high-resolution spectra of Au4f for HA-Au1 and HA-Au.

Abbreviations: TEM, transmission electron microscope; HA, hydroxyapatite; HA-Au, gold nanoparticles-loaded hydroxyapatite; XRD, X-ray powder diffractometry; FT-IR, fourier-transform infrared spectroscopy; XPS, X-ray photoelectron spectroscopy.

nanoparticles displayed a slight positive effect on cell proliferation of hMSCs during prolonged culture, when compared with the control groups. This might be explained by the good biological activity of AuNPs loaded on HA nanoparticles. Some other reports have revealed that AuNPs with different sizes can enhance cell viability and proliferation rate more than the control group.[26,28] Therefore, HA-Au2 nanoparticles at the concentration of 100 μg/mL were used for the rest of the studies.

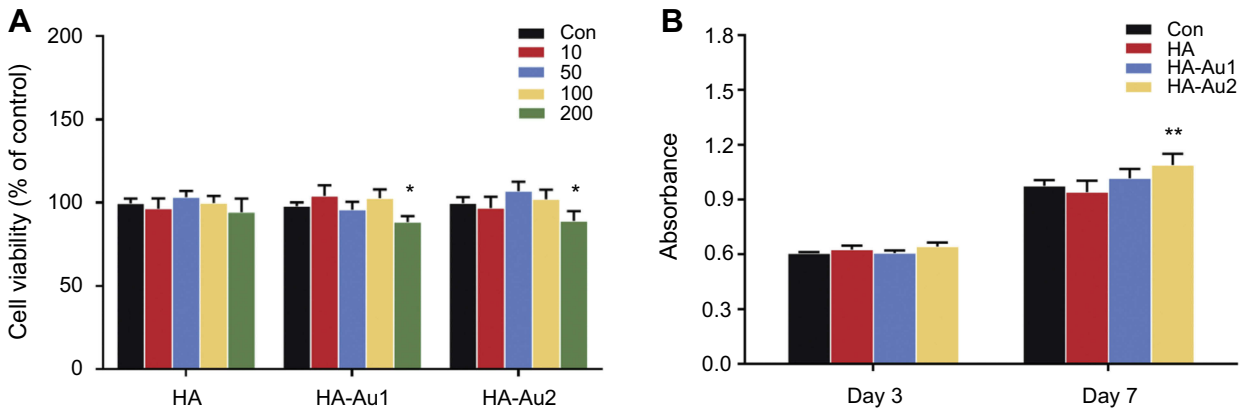

Figure 2 (**A**) Cell viability of hMSCs incubated with PBS (control), HA or HA-Au in growth medium at concentrations of 10, 50, 100, and 200 μg/mL for 2 days. (**B**) Cell proliferation of hMSCs incubated with PBS (control), HA or HA-Au in osteogenic induction medium at the concentration of 100 μg/mL for 3 and 7 days (*$p<0.05$, comparison between control group and other groups).

Abbreviations: hMSCs, human bone marrow-derived mesenchymal stem cells; HA, hydroxyapatite; HA-Au, gold nanoparticles-loaded hydroxyapatite.

To identify uptake of HA and HA-Au nanoparticles in hMSCs, the cells were cultured in the osteoinductive medium containing these nanoparticles for 3 days. As displayed in the TEM images (Figure 3A–D), the HA-Au nanoparticles were partially taken up by single hMSCs and internalized in the cell matrix. Most of the internalized HA and HA-Au nanoparticles were detected inside endosomal vesicles of hMSCs and did not enter the nucleolus. This result indicated that these nanoparticles entered the hMSCs through the endocytic pathway. Moreover, the

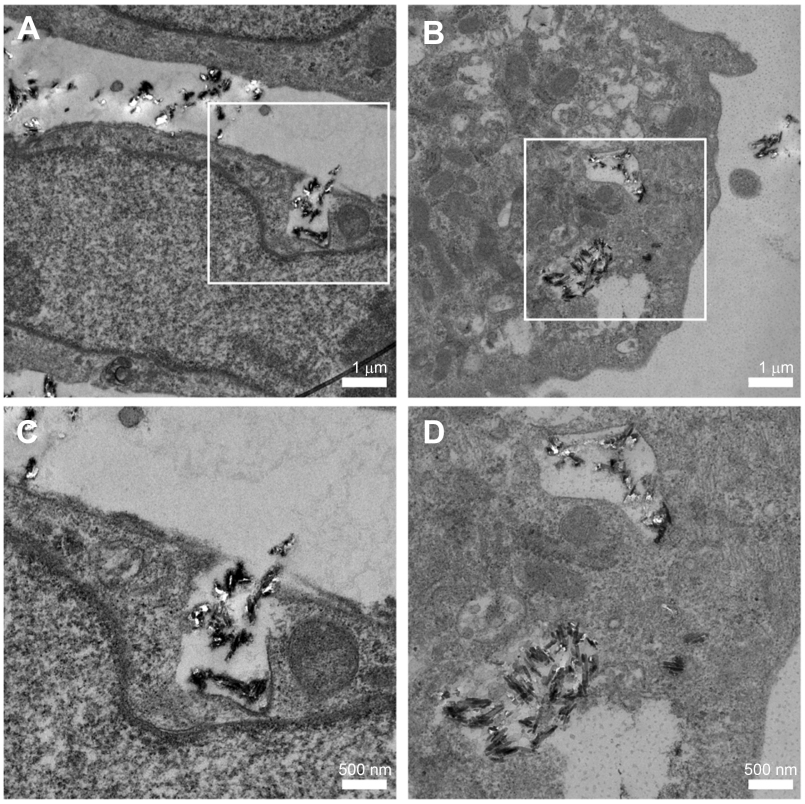

Figure 3 TEM images of HA (**A, C**) and HA-Au (**B, D**)-internalized hMSCs show that the particles can be uptaken by cells (black dots in white boxed areas in A and B (scale bar, 1 μm), with corresponding amplified images of **C** and **D** (scale bar, 500 nm).

Abbreviations: TEM, transmission electron microscope; hMSCs, human bone marrow-derived mesenchymal stem cells; HA, hydroxyapatite; HA-Au, gold nanoparticles-loaded hydroxyapatite.

cellular morphology and structures of cell organelles in hMSCs were not significantly affected by the internalized HA and HA-Au nanoparticles.

ALP production and calcium deposition

The ALP assay was conducted to evaluate if the HA-Au nanoparticles improved osteogenic differentiation activity in hMSCs. It has been reported that ALP is a specific marker during the early stage of osteogenic differentiation and generally reaches maximum expression level at 2 weeks.[35] Therefore, both quantitative and qualitative methods were used to measure ALP levels. After culturing in osteogenic induction medium containing HA and HA-Au nanoparticles for 3, 7, and 14 days, the hMSCs were collected for ALP staining and ALP activity assay. As shown in Figure 4A, the intensity of ALP staining in all groups was the highest after culturing for 14 days. During the early stage (3 days), the HA-Au nanoparticles-treated group did not show a significant difference in ALP staining compared with the HA group. However, the intensity of ALP staining in HA-Au nanoparticles-treated group was significantly higher than that of the HA group on day 7 and 14. These findings indicated that HA-Au nanoparticles exhibited more intense ALP staining than HA nanoparticles and controls during the 14-day experiments.

The ALP activity assay was performed in the same way as ALP activity. As expected, the ALP activity results revealed the similar trends as the ALP staining assay, as shown in Figure 4B. HA-Au nanoparticles-treated hMSCs had significantly higher ALP expression level than that of other groups. The HA-Au nanoparticles group expressed the highest ALP level. These results indicate that HA-Au nanoparticles could synergistically accelerate the osteogenic differentiation in hMSCs at an early stage.

Mineralized nodules were the final stage markers in the process of osteogenic differentiation.[36] Typically, when the cells started to mineralize, calcium depositions were formed and reached their maximum quantity after culturing for 2–3 weeks.[37] After culturing with or without HA and HA-Au nanoparticles in the osteoinductive medium for 14 and 21 days, the cells from each group were prepared for ARS staining in order to identify the mineralized nodules formation. As shown in Figure 5A, calcium deposition was expressed as red nodule-like staining. The amount of calcium deposition showed a continual increase during the 21-day period in all experimental groups. However, there was more mineralized nodule formation in hMSCs cultured with HA-Au nanoparticles than those in the HA and control groups, indicating that Au and HA nanoparticles had synergistic effects on calcium deposition. For quantitative analysis, we used the intensity of ARS extracted from the stained plates to confirm the calcium staining pattern (Figure 5B). The microplate reader was used to measure the optical density (O.D.) values of the corresponding sample. The HA-Au nanoparticles-treated group had the highest O.D. value. These results indicate that HA-Au nanoparticles strongly promote mineralization of hMSCs. In relation to this study,

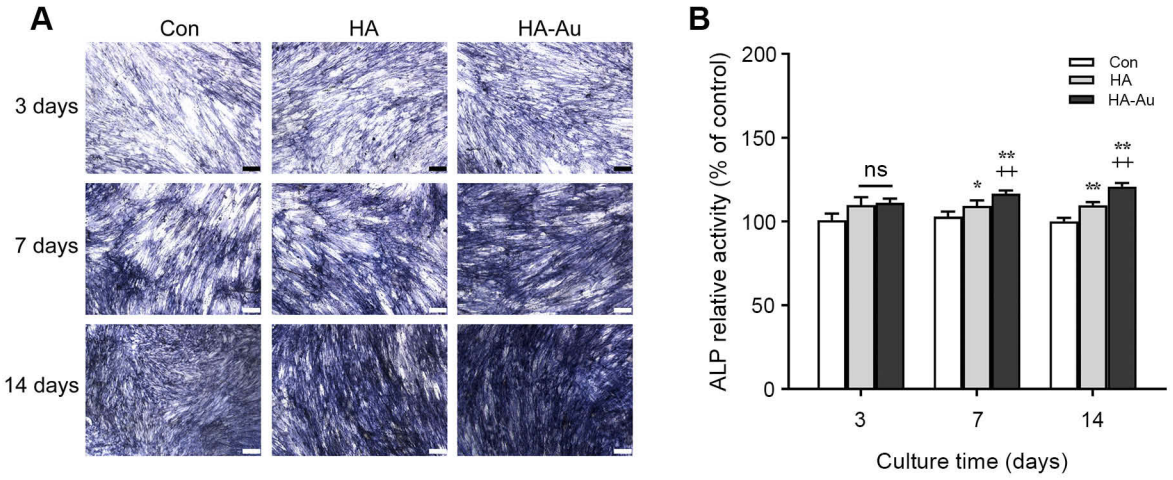

Figure 4 ALP staining (**A**) and ALP activity assay (**B**) of hMSCs after incubation with PBS (control), HA or HA-Au in osteogenic induction medium at the concentration of 100 μg/mL for 3, 7, and 14 days (scale bar: 100 μm. *p<0.05, **p<0.01, comparison between control group and other groups. ^{+}p<0.05, ^{++}p<0.01, comparison between HA group and HA-Au group).

Abbreviations: ALP, alkaline phosphatase; hMSCs, human bone marrow-derived mesenchymal stem cells; PBS, phosphate buffer saline; HA, hydroxyapatite; HA-Au, gold nanoparticles-loaded hydroxyapatite.

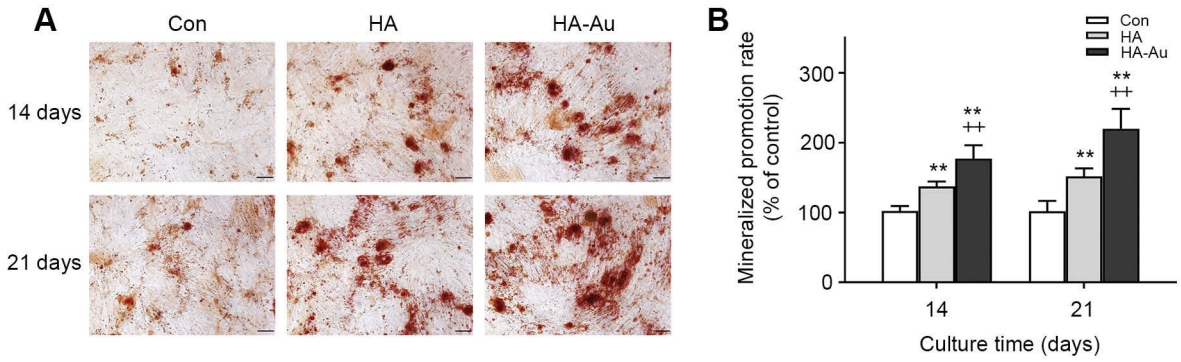

Figure 5 ARS staining (**A**) and calcium deposition assay (**B**) of hMSCs after incubation with PBS (control), HA or HA-Au in osteogenic induction medium at the concentration of 100 μg/mL for 14 and 21 days. (scale bar: 100 μm. *p<0.05, **p<0.01, comparison between control group and other groups. ^{+}p<0.05, ^{++}p<0.01, comparison between HA group and HA-Au group).

Abbreviations: ARS, Alizarin Red S; hMSCs, human bone marrow-derived mesenchymal stem cells; PBS, phosphate buffer saline; HA, hydroxyapatite; HA-Au, gold nanoparticles-loaded hydroxyapatite.

a recent report indicated that calcium phosphate containing gold nanoparticles (GNP-CPC) displayed significant positive effects in the promotion of osteogenic differentiation by increasing the ALP activity and mineralized nodules of hDPSCs.[38]

Osteogenic gene expression

Osteogenic differentiation is a complex biological process involving the expression of several regulated genes and specific marker genes at different stages. For a more analytical approach, the effects of HA-Au nanoparticles on bone sialoprotein (BSP), and collagen type I (COL1), ALP, runt-related transcription factor 2 (Runx2) osteopontin (OPN) and osteocalcin (OCN) mRNA expression levels in hMSCs were measured. Runx2, an osteogenesis-related transcriptional factor, was able to initiate osteogenic differentiation and activate other osteogenesis-related genes and phenotypic markers.[39] COL1 was formed during the proliferation of osteoblasts and played an important role in bone matrix.[40] ALP, another crucial regulator of early stage osteogenic differentiation, initiated the progress of mineralization and gradually decreased in expression during the later stages of differentiation.[41] BSP, an indicator of osteogenesis, played an active role in promoting bone formation.[42] OCN and OPN were key markers of calcium deposition in the extracellular matrix and mineralization during the late stage of osteogenic differentiation.[43] After 3 and 7 days, mRNA expression of these osteogenesis-related genes was significantly enhanced in the HA-Au nanoparticles-treated groups (Figure 6). Compared with HA-Au groups, three of the osteogenic markers (COL1, ALP, OCN) in the HA groups did not show significant differences in expression during the early stages (3 days). However, over a prolonged period (7 days), as Au nanoparticles began to function, the expression levels of the genes examined in hMSCs treated with HA-Au nanoparticles were significantly higher than those in the pure HA group.

Based on integrated real-time PCR results, HA-Au nanocomposites proved to synergistically promote osteogenic differentiation in hMSCs, as reflected by the high expression levels of typical osteogenesis-related genes. Another recent study widely investigated composite biomaterials based on AuNPs and HA nanoparticles. miR-29b-loaded AuNPs were developed as a delivery system for synergistically promoting osteoblastic differentiation.[44] HA-based composites (HA-gelatin-chitosan-fibrin-bone ash) have been synthesized and characterized for bone tissue engineering applications.[9]

Effects of HA-Au nanoparticles on the Wnt/b-catenin signal pathway

Recent evidence showed that mechanical stimuli from nanoparticles may regulate the direction of stem cells differentiation via activating related signaling pathways.[22,45] It has been reported that Wnt/β-catenin signaling pathway, which plays an important role in the process of osteogenic differentiation of stem cells, can be activated by mechanical stimulation.[46–48] Therefore, the HA-Au nanoparticles may serve as mechanical stimuli to induce the differentiation of hMSCs to osteoblasts via activating the Wnt/β-catenin signaling pathway. In this study, β-catenin was identified as a crucial regulator in this signaling pathway using Western blotting experiments and real-time PCR assays. As shown in Figure 7A–C, using Western blot and real-time PCR

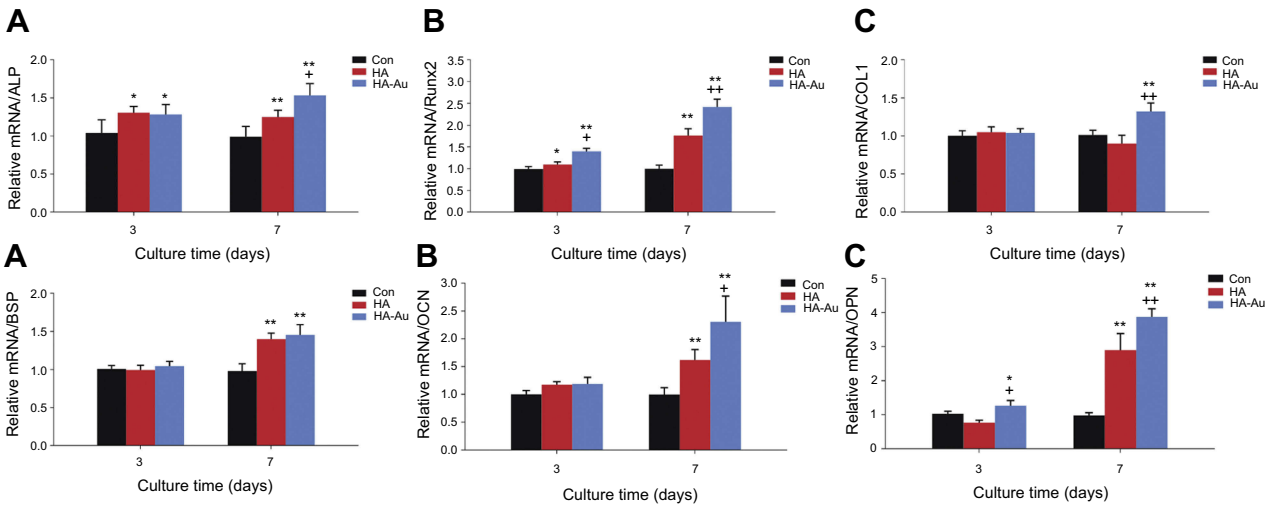

Figure 6 The expression of osteogenic differentiation specific genes in hMSCs after incubation with PBS (control), HA or HA-Au in osteogenic induction medium at the concentration of 100 μg/mL for 3 and 7 days: ALP (**A**), Runx2 (**B**), COL1 (**C**), BSP (**D**), OCN (**E**) and, OPN (**F**). (*p<0.05, **p<0.01, comparison between control group and other groups. ^{+}p<0.05, ^{++}p<0.01, comparison between HA group and HA-Au group).

Abbreviations: hMSCs, human bone marrow-derived mesenchymal stem cells; PBS, phosphate buffer saline; HA, hydroxyapatite; HA-Au, gold nanoparticles-loaded hydroxyapatite; ALP, alkaline phosphatase; Runx2, runt-related transcription factor 2; COL1, collagen type Ⅰ; BSP, bone sialoprotein; OCN, osteocalcin; OPN, osteopontin.

evaluation we found that HA-Au nanoparticles significantly enhanced the expression of β-catenin in hMSCs. The non-phosphorylated β-catenin protein tended to transfer into the nucleus and combine with target genes, thus regulating the Wnt/β-catenin signaling pathway.[49,50] Further studies showed that HA-Au nanoparticles dramatically increased expression levels of the downstream molecule axin-2 (Figure 7D). These results suggest that Wnt/b-catenin signal pathway is involved in the process of osteogenic differentiation in hMSCs induced by HA-Au nanoparticles.

In addition, we investigated whether the osteogenic effect of HA-Au nanoparticles was mediated via modification of Wnt/b-catenin signal pathway. The hMSCs were pretreated with the Wnt/β-catenin signaling pathway inhibitor ICG-001, and subsequently co-cultured with HA-Au nanoparticles for further osteogenic differentiation. As expected, ICG-001 reversed the HA-Au nanoparticles-induced enhancement of β-catenin activity (Figure 7E–H). In accordance with this result, the enhanced osteogenic differentiation by HA-Au

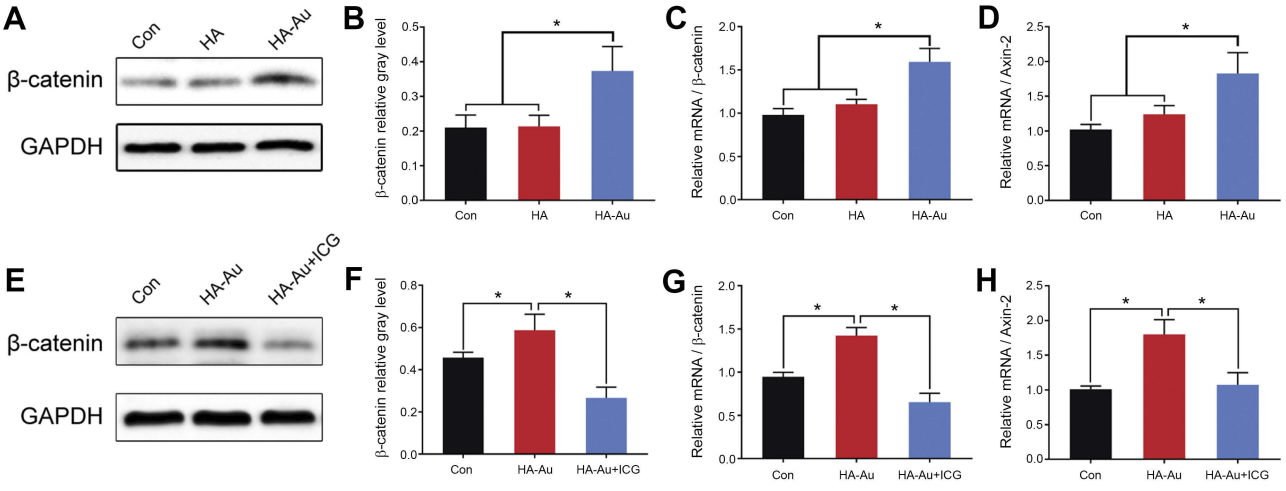

Figure 7 Western blot and RT-PCR results showed that HA-Au increased the expression of β-catenin and β-catenin target gene axin-2 in hMSCs (**A**–**D**). Meanwhile, β-catenin and axin-2 expression levels were significantly reduced when ICG-001 was added (**E**–**H**). (*p<0.05, **p<0.01, comparison between control group and other groups).

Abbreviations: RT-PCR, real-time polymerase chain reaction; hMSCs, human bone marrow-derived mesenchymal stem cells; HA, hydroxyapatite; HA-Au, gold nanoparticles-loaded hydroxyapatite.

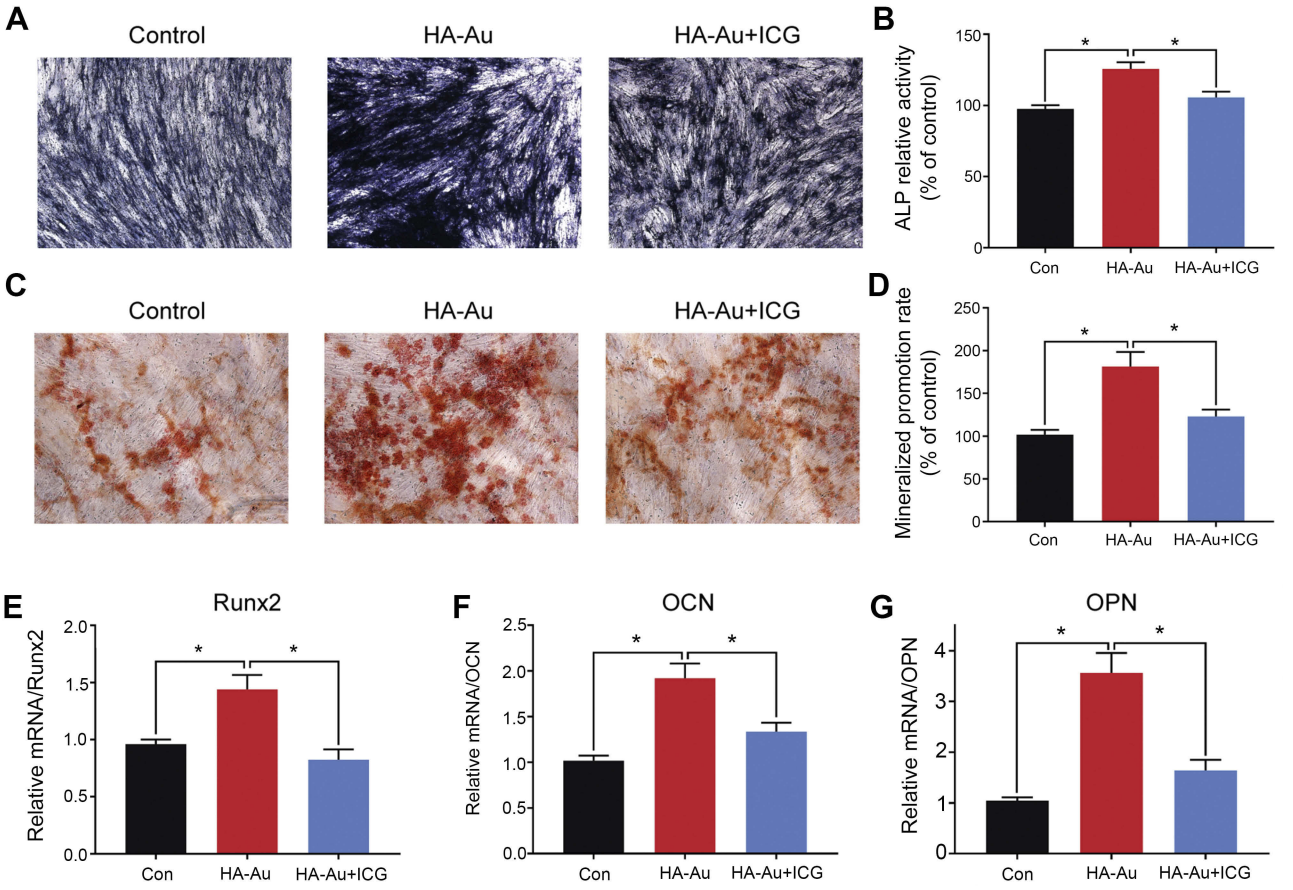

Figure 8 Wnt/β-catenin inhibitor reversed effects of HA-Au on osteogenic differentiation of hMSCs. hMSCs osteogenic differentiation was assessed by ALP staining (**A, B**) and ARS staining (**C, D**) after culture for 7 and 21 days, respectively. The mRNA levels of Runx2 (**E**), OCN (**F**) and OPN (**G**) were determined by RT-PCR. (*$p<0.05$, **$p<0.01$, comparison between the control group and other groups).

Abbreviations: hMSCs, human bone marrow-derived mesenchymal stem cells; HA, hydroxyapatite; HA-Au, gold nanoparticles-loaded hydroxyapatite; ALP, alkaline phosphatase; ARS, Alizarin Red S; Runx2, runt-related transcription factor 2; OCN, osteocalcin; OPN, osteopontin; RT-PCR, real-time polymerase chain reaction.

nanoparticles was significantly inhibited when ICG-001 was administered (Figure 7). These results revealed that ALP production and calcium deposition in hMSCs treated with HA-Au nanoparticles dramatically decreased after the addition of ICG-001 (Figure 8A–D). Moreover, ICG-001 also abolished the nanoparticles-mediated promotion of the expression of Runx-2, OCN, and OPN (Figure 8E–G). Collectively, these observations strongly suggest that the enhanced osteogenic differentiation of hMSCs by HA-Au nanoparticles might be regulated via the Wnt/b-catenin signaling pathway. Furthermore, the positive effects of HA-Au nanoparticles on osteogenic differentiation in hMSCs were inhibited following ICG-001 administration.

Conclusion

In the present study, a novel HA-Au nanoparticle composites were developed and its in vitro biocompatibility and osteogenic induction effect in hMSCs was assessed for the first time. Although the underlying mechanism has not yet been confirmed, the results indicate that HA-Au nanoparticles can be internalized into hMSCs to activate the Wnt/β-catenin signaling pathway, leading to the acceleration of osteogenic differentiation in hMSCs. However, a more detailed mechanism and the in vivo efficacy are still obscure and require further investigation. In conclusion, this study suggests that HA-Au nanocomposites can be potential candidates for scaffolding in bone tissue regeneration.

Acknowledgment

This work was supported by National Key Research and Development Program of China (2018YFB1105700).

Disclosure

The authors report no conflicts of interest in this work.

References

1. Naveena N, Venugopal J, Rajeswari R, et al. Biomimetic composites and stem cells interaction for bone and cartilage tissue regeneration. *J Mater Chem*. 2012;22(12):5239–5253. doi:10.1039/c1jm14401d
2. Marcucio RS, Nauth A, Giannoudis PV, et al. Stem cell therapies in orthopaedic trauma (vol 29, pg S24, 2015). *J Orthop Trauma*. 2016;30(2):E74–E74. doi:10.1097/BOT.0000000000000535
3. Gong T, Xie J, Liao J, Zhang T, Lin S, Lin Y. Nanomaterials and bone regeneration. *Bone Res*. 2015;3:15029. doi:10.1038/boneres.2015.29
4. Shanmuganathan R, Edison T, LewisOscar F, Kumar P, Shanmugam S, Pugazhendhi A. Chitosan nanopolymers: an overview of drug delivery against cancer. *Int J Biol Macromol*. 2019;130:727–736. doi:10.1016/j.ijbiomac.2019.02.060
5. Tautzenberger A, Kovtun A, Ignatius A. Nanoparticles and their potential for application in bone. *Int J Nanomedicine*. 2012;7:4545–4557. doi:10.2147/IJN.S34127
6. Pugazhendhi A, Edison T, Karuppusamy I, Kathirvel B. Inorganic nanoparticles: a potential cancer therapy for human welfare. *Int J Pharm*. 2018;539(1–2):104–111. doi:10.1016/j.ijpharm.2018.01.034
7. Lee JH, Shin YC, Lee SM, et al. Enhanced osteogenesis by reduced graphene oxide/hydroxyapatite nanocomposites. *Sci Rep*. 2015;5:18833. doi:10.1038/srep18833
8. Huebsch N, Mooney DJ. Inspiration and application in the evolution of biomaterials. *Nature*. 2009;462(7272):426–432. doi:10.1038/nature08601
9. Sathiyavimal S, Vasantharaj S, LewisOscar F, Pugazhendhi A, Subashkumar R. Biosynthesis and characterization of hydroxyapatite and its composite (hydroxyapatite-gelatin-chitosan-fibrin-bone ash) for bone tissue engineering applications. *Int J Biol Macromol*. 2019;129:844–852. doi:10.1016/j.ijbiomac.2019.02.058
10. Zhou H, Lee J. Nanoscale hydroxyapatite particles for bone tissue engineering. *Acta Biomater*. 2011;7(7):2769–2781. doi:10.1016/j.actbio.2011.03.019
11. Remya KR, Joseph J, Mani S, John A, Varma HK, Ramesh P. Nanohydroxyapatite incorporated electrospun polycaprolactone/polycaprolactone-polyethyleneglycol-polycaprolactone blend scaffold for bone tissue engineering applications. *J Biomed Nanotechnol*. 2013;9(9):1483–1494.
12. Shi Z, Huang X, Cai Y, Tang R, Yang D. Size effect of hydroxyapatite nanoparticles on proliferation and apoptosis of osteoblast-like cells. *Acta Biomater*. 2009;5(1):338–345. doi:10.1016/j.actbio.2008.07.023
13. Gao P, Zhang HQ, Liu Y, et al. Beta-tricalcium phosphate granules improve osteogenesis in vitro and establish innovative osteo-regenerators for bone tissue engineering in vivo. *Sci Rep*. 2016;6:23367. doi:10.1038/srep23367
14. Chellapandian C, Ramkumar B, Puja P, Shanmuganathan R, Pugazhendhi A, Kumar P. Gold nanoparticles using red seaweed Gracilaria verrucosa: green synthesis, characterization and biocompatibility studies. *Process Biochem*. 2019;80:58–63. doi:10.1016/j.procbio.2019.02.009
15. Li J, Zheng L, Cai H, et al. Facile one-pot synthesis of Fe3O4@Au composite nanoparticles for dual-mode MR/CT imaging applications. *ACS Appl Mater Interfaces*. 2013;5(20):10357–10366. doi:10.1021/am4034526
16. Murphin Kumar PS, MubarakAli D, Saratale RG, et al. Synthesis of nano-cuboidal gold particles for effective antimicrobial property against clinical human pathogens. *Microb Pathog*. 2017;113:68–73. doi:10.1016/j.micpath.2017.10.032
17. Hutter E, Boridy S, Labrecque S, et al. Microglial response to gold nanoparticles. *ACS Nano*. 2010;4(5):2595–2606. doi:10.1021/nn901869f
18. Khlebtsov N, Bogatyrev V, Dykman L, et al. Analytical and theranostic applications of gold nanoparticles and multifunctional nanocomposites. *Theranostics*. 2013;3(3):167–180. doi:10.7150/thno.5716
19. Orza A, Soritau O, Olenic L, et al. Electrically conductive gold-coated collagen nanofibers for placental-derived mesenchymal stem cells enhanced differentiation and proliferation. *ACS Nano*. 2011;5(6):4490–4503. doi:10.1021/nn1035312
20. Liu X, Huang H, Liu G, et al. Multidentate zwitterionic chitosan oligosaccharide modified gold nanoparticles: stability, biocompatibility and cell interactions. *Nanoscale*. 2013;5(9):3982–3991. doi:10.1039/c3nr00284e
21. Pissuwan D, Niidome T, Cortie MB. The forthcoming applications of gold nanoparticles in drug and gene delivery systems. *J Control Release*. 2011;149(1):65–71. doi:10.1016/j.jconrel.2009.12.006
22. Yi C, Liu D, Fong CC, Zhang J, Yang M. Gold nanoparticles promote osteogenic differentiation of mesenchymal stem cells through p38 MAPK pathway. *ACS Nano*. 2010;4(11):6439–6448. doi:10.1021/nn101373r
23. Choi SY, Song MS, Ryu PD, Lam AT, Joo SW, Lee SY. Gold nanoparticles promote osteogenic differentiation in human adipose-derived mesenchymal stem cells through the Wnt/beta-catenin signaling pathway. *Int J Nanomedicine*. 2015;10:4383–4392. doi:10.2147/IJN.S78775
24. Zhang D, Liu D, Zhang J, Fong C, Yang M. Gold nanoparticles stimulate differentiation and mineralization of primary osteoblasts through the ERK/MAPK signaling pathway. *Mater Sci Eng C Mater Biol Appl*. 2014;42:70–77. doi:10.1016/j.msec.2014.04.042
25. Yao Y, Shi X, Chen F. The effect of gold nanoparticles on the proliferation and differentiation of murine osteoblast: a study of MC3T3-E1 cells in vitro. *J Nanosci Nanotechnol*. 2014;14(7):4851–4857. doi:10.1166/jnn.2014.8717
26. Ko WK, Heo DN, Moon HJ, et al. The effect of gold nanoparticle size on osteogenic differentiation of adipose-derived stem cells. *J Colloid Interface Sci*. 2015;438:68–76. doi:10.1016/j.jcis.2014.08.058
27. Li J, Li JJ, Zhang J, Wang X, Kawazoe N, Chen G. Gold nanoparticle size and shape influence on osteogenesis of mesenchymal stem cells. *Nanoscale*. 2016;8(15):7992–8007. doi:10.1039/c5nr08808a
28. Zhang Y, Kong N, Zhang Y, Yang W, Yan F. Size-dependent effects of gold nanoparticles on osteogenic differentiation of human periodontal ligament progenitor cells. *Theranostics*. 2017;7(5):1214–1224. doi:10.7150/thno.17252
29. Xu X, Liu X, Tan L, et al. Controlled-temperature photothermal and oxidative bacteria killing and acceleration of wound healing by polydopamine-assisted Au-hydroxyapatite nanorods. *Acta Biomater*. 2018;77:352–364. doi:10.1016/j.actbio.2018.07.030
30. Liu X, Man HC. Laser fabrication of Ag-HA nanocomposites on Ti6Al4V implant for enhancing bioactivity and antibacterial capability. *Mater Sci Eng C Mater Biol Appl*. 2017;70(Pt 1):1–8. doi:10.1016/j.msec.2016.08.059
31. Wang Z, Dong CF, Yang SF, Zhang DW, Xiao K, Li XG. Facile incorporation of hydroxyapatite onto an anodized Ti surface via a mussel inspired polydopamine coating. *Appl Surf Sci*. 2016;378:496–503. doi:10.1016/j.apsusc.2016.03.094
32. Zhou YZ, Cao Y, Liu W, Chu CH, Li QL. Polydopamine-induced tooth remineralization. *ACS Appl Mater Interfaces*. 2012;4(12):6900–6909. doi:10.1021/am302041b
33. Lee JH, Shin YC, Jin OS, et al. Reduced graphene oxide-coated hydroxyapatite composites stimulate spontaneous osteogenic differentiation of human mesenchymal stem cells. *Nanoscale*. 2015;7(27):11642–11651. doi:10.1039/c5nr01580d
34. Khajuria DK, Kumar VB, Gigi D, Gedanken A, Karasik D. Accelerated bone regeneration by nitrogen-doped carbon dots functionalized with hydroxyapatite nanoparticles. *ACS Appl Mater Interfaces*. 2018;10(23):19373–19385. doi:10.1021/acsami.8b02792
35. Liu D, Yi C, Zhang D, Zhang J, Yang M. Inhibition of proliferation and differentiation of mesenchymal stem cells by carboxylated carbon nanotubes. *ACS Nano*. 2010;4(4):2185–2195. doi:10.1021/nn901479w
36. Ravichandran R, Venugopal JR, Sundarrajan S, Mukherjee S, Ramakrishna S. Precipitation of nanohydroxyapatite on PLLA/PBLG/Collagen nanofibrous structures for the differentiation of adipose derived stem cells to osteogenic lineage. *Biomaterials*. 2012;33(3):846–855. doi:10.1016/j.biomaterials.2011.10.030

37. Stein GS, Lian JB. Molecular mechanisms mediating proliferation/differentiation interrelationships during progressive development of the osteoblast phenotype. *Endocr Rev*. 1993;14(4):424–442. doi:10.1210/edrv-14-4-424
38. Xia Y, Chen H, Zhang F, et al. Gold nanoparticles in injectable calcium phosphate cement enhance osteogenic differentiation of human dental pulp stem cells. *Nanomedicine*. 2018;14(1):35–45. doi:10.1016/j.nano.2017.08.014
39. Long F. Building strong bones: molecular regulation of the osteoblast lineage. *Nat Rev Mol Cell Biol*. 2011;13(1):27–38. doi:10.1038/nrm3254
40. Komori T. Requisite roles of Runx2 and Cbfb in skeletal development. *J Bone Miner Metab*. 2003;21(4):193–197. doi:10.1007/s00774-002-0408-0
41. Marie PJ. Transcription factors controlling osteoblastogenesis. *Arch Biochem Biophys*. 2008;473(2):98–105. doi:10.1016/j.abb.2008.02.030
42. Frank O, Heim M, Jakob M, et al. Real-time quantitative RT-PCR analysis of human bone marrow stromal cells during osteogenic differentiation in vitro. *J Cell Biochem*. 2002;85(4):737–746. doi:10.1002/jcb.10174
43. Dhore CR, Cleutjens JP, Lutgens E, et al. Differential expression of bone matrix regulatory proteins in human atherosclerotic plaques. *Arterioscler Thromb Vasc Biol*. 2001;21(12):1998–2003.
44. Pan T, Song W, Gao H, et al. miR-29b-loaded gold nanoparticles targeting to the endoplasmic reticulum for synergistic promotion of osteogenic differentiation. *ACS Appl Mater Interfaces*. 2016;8(30):19217–19227. doi:10.1021/acsami.6b02969
45. Yang K, Cao W, Hao X, et al. Metallofullerene nanoparticles promote osteogenic differentiation of bone marrow stromal cells through BMP signaling pathway. *Nanoscale*. 2013;5(3):1205–1212. doi:10.1039/c2nr33575a
46. Robinson JA, Chatterjee-Kishore M, Yaworsky PJ, et al. Wnt/beta-catenin signaling is a normal physiological response to mechanical loading in bone. *J Biol Chem*. 2006;281(42):31720–31728. doi:10.1074/jbc.M602308200
47. Case N, Ma MY, Sen B, Xie ZH, Gross TS, Rubin J. Beta-catenin levels influence rapid mechanical responses in osteoblasts. *J Biol Chem*. 2008;283(43):29196–29205. doi:10.1074/jbc.M801907200
48. Sen B, Xie ZH, Case N, Ma MY, Rubin C, Rubin J. Mechanical strain inhibits adipogenesis in mesenchymal stem cells by stimulating a durable beta-catenin signal. *Endocrinology*. 2008;149(12):6065–6075. doi:10.1210/en.2008-0687
49. Clevers H. Wnt/beta-catenin signaling in development and disease. *Cell*. 2006;127(3):469–480. doi:10.1016/j.cell.2006.10.018
50. Takahashi-Yanaga F, Sasaguri T. The Wnt/beta-catenin signaling pathway as a target in drug discovery. *J Pharmacol Sci*. 2007;104(4):293–302.